PROCEEDINGS OF SCIENCE

Antiproton-proton interaction and related hadron physics

Xian-Wei Kang*
Institute for Advanced Simulation, Jülich Center for Hadron Physics, and Institut für Kernphysik, Forschungszentrum Jülich, D-52425 Jülich, Germany
E-mail: x.kang@fz-juelich.de

Antinucleon-nucleon interaction has been established in chiral effective field theory. The strong threshold enhancement observed in the reactions $J/\psi \to \gamma\bar{p}p$ and $e^+e^- \to \bar{p}p$ are interpreted by the strong $\bar{p}p$ interaction. Concerning the channel $J/\psi \to \gamma\bar{p}p$, the topic on the $\bar{p}p$ bound state is also discussed.

*The 8th International Workshop on Chiral Dynamics, CD2015 ****
29 June 2015 - 03 July 2015
Pisa,Italy

*Speaker.

PoS(CD15)108

1. Introduction

Few-body hadron-hadron interaction has been and is still a fundemantal constituent part of hadron and nuclear physics. Among them, the antinucleon-nucleon ($\overline{N}N$) has been achieved fruitful progress, especially in a meson-exchange model, see e.g., a review in Ref. [1]. And after 1990s, chiral effective field theory (EFT) has become a powerful tool to analyze nucleon-nucleon interaction, for a review, see e.g., Ref. [2]. However, only little work of $\overline{N}N$ in chiral EFT has been done, besides the one of partial-wave analysis (PWA) [3]. The recently resurgent interest of $\bar{p}p$ physics is triggered by the threshold enhancement in $\bar{p}p$ invariant mass spectrum observed in experiments, e.g, for the decays $J/\psi \to \gamma\bar{p}p$ [4, 5], $e^+e^- \to \bar{p}p$ [6, 7]. We will elaborate below how we use the $\bar{p}p$ final-state interaction (FSI) to interpret these phenomenons.

2. $\overline{N}N$ interaction in chiral EFT

$\overline{N}N$ potential consists of two parts: elastic scattering part and the annihilation, which is the same feature in the framework of both the conventional meson-exchange model and the chiral EFT. The difference is on the technical treatment. In chiral EFT, the elastic part is governed by the pion exchanges (pion as the only degree of freedom in chiral EFT), which is tied closely to the knowledge of NN interaction except for the sign difference due to the $G-$parity transformation (see e.g., Ref. [8]). For the power counting rule and details in NN scattering, one refers to Ref. [2]. Here we only remind that

$$V_{1\pi}^{\bar{N}N} = -V_{1\pi}^{NN}\,, \quad V_{2\pi}^{\bar{N}N} = V_{2\pi}^{NN} \tag{2.1}$$

because of the $G-$parity transformation rule from πNN vertex to $\pi\overline{N}\overline{N}$. The new feature of $\overline{N}N$ compared to NN is the existence of annihilation effect that will be parameterised in contact term (in charge of short-range interaction). In Jülich model [9], the annihilation is treated as a energy-, spin-, and isospin-independent Gaussian form. Here we still follow the spirit of chiral power counting, taking ${}^1S_0$ partial wave as example. Starting form the most elaborated couple-channel model, we have

$$V_{\rm ann} = \sum_{X=2\pi,3\pi,\ldots} V_{\overline{N}N\to X} G_X(z) V_{X\to\overline{N}N}, \tag{2.2}$$

where X denotes, in principle, any possible intermediate states including $2\pi, 3\pi,$ etc., and G is the free Green's function. It is argued that the annihilation does not introduce a new scale into the problem [10], i.e., it can be likewise treated in the chiral expansion. Then up to next-to-next-to-leading order (NNLO), one can write the $\overline{N}N \to i$ (i as mesons) annihilation potential in ${}^1S_0$ partial wave as

$$V_{\overline{N}N\to i} = a_i + b_i p^2, \tag{2.3}$$

where $p\,(p')$ is the module of three-momentum in center-of-mass system (CMS) of intital (final) $\overline{N}N$ states. Picking out the imaginary part, one would get

$$\mathrm{Im}\, V_{\rm ann}({}^1S_0) = -\left(\tilde{C}^a_{{}^1S_0} + C^a_{{}^1S_0} p^2\right)\left(\tilde{C}^a_{{}^1S_0} + C^a_{{}^1S_0} p'^2\right). \tag{2.4}$$

Equation (2.4) fulfils the unitary condition by definition (an alternative method is based on the dispersion theory, see e.g., the $\pi\pi$ sector in Ref. [11]). Expanding the real part from the principal-value integral, we will get the similar structure as the NN case,

$$\mathrm{Re}\,V_{\mathrm{ann}}(^1S_0) = \tilde{C}_{^1S_0} + C_{^1S_0}\left(p^2 + p'^2\right). \tag{2.5}$$

Note there are four LECs ($\tilde{C}^a_{^1S_0}, C^a_{^1S_0}, \tilde{C}_{^1S_0}, C_{^1S_0}$) in total, where the annihilation in indicated in the superscript by "a". Now the $\overline{N}N$ potential is setting up but containing the low-energy constants (LECs). The recent energy-dependent $\overline{N}N$ partial-wave analysis (PWA) is done in Ref. [3], which provides a rather nice description of all the $\bar{p}p$ scattering data below laboratory momentum of 925 MeV. These LECs will be fitted to the partial-wave amplitude there. The results for the inelasticity and phase shfits of $^{11}S_0$ are shown in Fig. 1 up to $T_{\mathrm{lab}} = 200$ MeV for NLO and $T_{\mathrm{lab}} = 250$ MeV for NNLO. T_{lab} is the kinetic laboratory energy, $T_{\mathrm{lab}} = 2k^2/m$ with k denoting the module of the on-shell momentum in CMS. We have used the notation $^{2I+1\,2S+1}L_J$, where L, S, J denote the orbital angular momentum, total spin and their quantum addition, i.e, total angular momentum, respectively. The phase shift (complex value due to annihilation) is defined from $S-$matrix as $S = \eta e^{2i\delta_R} \equiv e^{2i\delta}$ with $\delta \equiv \delta_R + i\delta_I$, and then $\delta_I = -\log(\eta)/2$. The band is formed by varying the cutoff combination applied into the Lippmann-Schwinger equation and spectral function in the two-pion exchange potential [12, 10]. From Fig. 1 one sees that our results reproduce the PWA rather well with very small uncertainty (cutoff dependence) at the whole region considered. The corresponding results for coupled partial wave $^3S_1 - {}^3D_1$ will be used in the following subsection but are not shown here due to the limited space. For the reader who is interested in this part, one refers to the publication in [10]. Besides the phase shifts and inelasticities, the scattering length, and the level shifts and widths of the antiprotonic hydrogen are also calculated. They are all in good agreement with experimental numbers within error bars. $\overline{N}N$ Bound states are predicted in $^{13}P_0$ and $^{13}S_1 - {}^{13}D_1$ partial waves [10].

3. $\bar{p}p$ related hadron physics

3.1 $\bar{p}p$-threshold enhancement in $J/\psi \to \gamma\bar{p}p$

After the discovery of the strong threshold enhancement observed in $J/\psi \to \gamma\bar{p}p$ by BES collaboration [4], many explanations have been proposed. Due to its proximity to $\bar{p}p$ threshold, it is speculated to be a $\bar{p}p$ bound state, or at least, has much to do with $\bar{p}p$ interaction. To take into account the $\bar{p}p$ FSI, we write the total amplitude symbolically as

$$A = A_0 + A_0 G T_{\bar{p}p}, \tag{3.1}$$

where A_0 is the elementary production amplitude without considering $\bar{p}p$ FSI, and in the second term the off-shell form for A_0 is needed since it appears in the integral; G is the free $\bar{p}p$ Green's function; the T-matrix elements, $T_{\bar{p}p}$, can be calculated from Sec. 2. Writing Eq. (3.1) in a partial wave more explicitly, one gets (here for $S-$wave)

$$A_L = A_L^0\left[1 + \int_0^\infty \frac{dqq^2}{(2\pi)^3}\frac{1}{2E_k - 2E_q + i0^+}T_L(q,k;E_k)\right]. \tag{3.2}$$

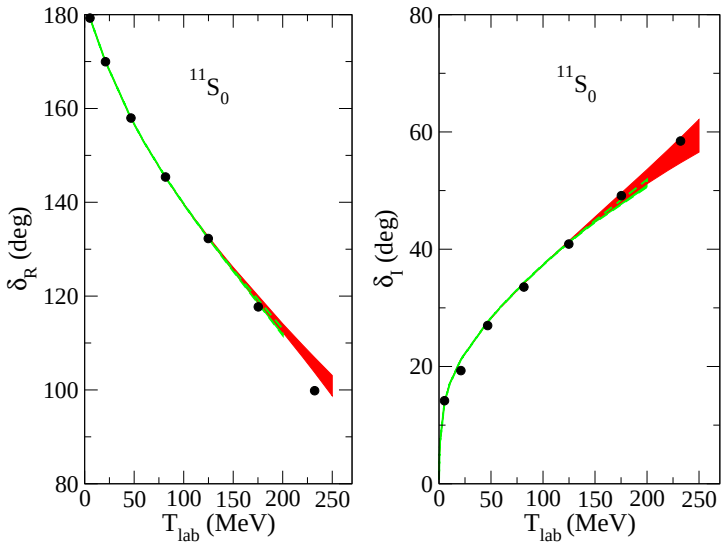

Figure 1: Complex phase shifts for isospin-0 $^1S_0$ $\left(^{11}S_0\right)$ partial wave in unit of degree as a function of kinetic laboratory energy $T_{\rm lab}$. δ_R coincides with the widely used conventional real phase shift while $\delta_I = -\log(\eta)/2$. Circle points represent PWA reported from Ref. [3]. Green (Red) band indicates the cutoff dependence of NLO (NNLO) potential.

At low-energy region, assuming A_0 has only a weak energy dependence, one may reasonably approximate as a constant. In this way, in the model there will be only one parameter, i.e., the overall normalization constant. For the observable of event distribution, we are doing a parameter-free calculation, as a matter of fact, in viewpoint of only the energy dependence. We stress that the energy dependence of this whole system solely comes from $\bar{p}p$ interaction since A_0 is treated as a constant. This point indeed verifies the momentous role of $\bar{p}p$ FSI. In the channel $e^+e^- \to \bar{p}p$, see Sec. 3.2, the overall constant is used to match the magnitude of the cross section. In the process $J/\psi \to \gamma\bar{p}p$, the lowest allowed quantum number for $\bar{p}p$ is $^1S_0$, and both isospin-0 and 1 are allowed. The result based on the original $^1S_0$ potential constrained by PWA of Ref. [3] does not reproduce such a strong enhanced peak near $\bar{p}p$ threshold. Instead, we perform a combined analysis of the $\bar{p}p$ scattering data as well as the prominent peak shown by BES data [5]. T-matrix is taken as $T = (T^0 + T^1)/2$, where the superscript denotes isospin. The LECs for isospin-0 $^1S_0$ is kept as what comes from fitting to the PWA of Ref. [3], supported by the milder energy dependence of $J/\psi \to \omega\bar{p}p$ [13], while the four LECs in isospin-1 $^1S_0$ is refitted. So in total, there are 5 free parameters (4 LECs + 1 overall constant). The results are presented in Fig. 2 and Fig. 3. One can see that the peak around $\bar{p}p$ threshold is nicely reproduced, and simultaneously, the $^1S_0$ partial-wave cross section of the PWA as well the original one constructed by us but fitted to PWA are very well reproduced. Then the total cross section from our potential (only $^{31}S_0$ part changes and others do not alter compared to Ref. [10]) is thus expected to be in a good agreement with the one calculated from PWA. The protonium level shift and widths are also examined, and they are also within experimental error bars. It turns that in order to describe such a prominent peak, we need a $\bar{p}p$ bound state in isospin-1 $^1S_0$. Note that the analysis of these data utilizing the Paris $\overline{N}N$ potential suggests isospin I=0 for this $^1S_0$ quasibound state [15]. However, one should keep in mind that the data above threshold

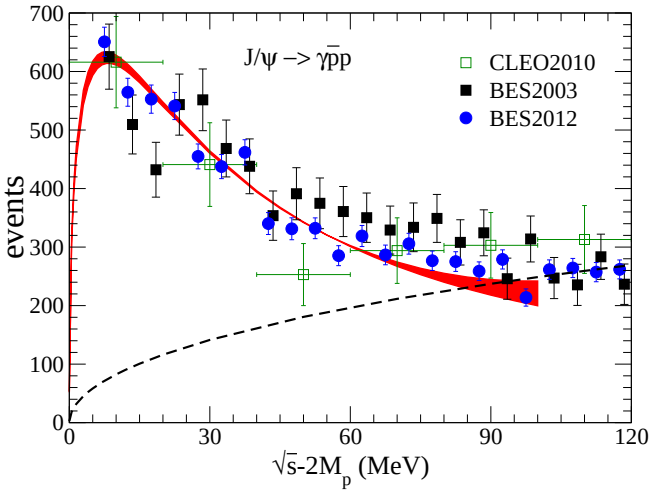

Figure 2: $\bar{p}p$ spectrum for the decay $J/\psi \to \gamma\bar{p}p$. The band represents our result. The dashed curve denotes the phase space behavior. Data are taken from Refs. [4, 5, 14]. The measurement of Ref. [5] is adopted for the scale. The data for the BES measurement from 2003 have been shifted 1 MeV to the right to discriminate from the new measurement.

is believed to be not capable of pinning down the binding energy and width of this bound state. More information on the invariant mass spectrum below $\bar{p}p$ threshold is needed. In Ref. [16], the systematic description of the $\bar{p}p$ mass spectrum in other J/ψ and ψ' decays are achieved. In our calculation, the mass difference of proton and neutron, as well as the Coulomb interaction is not considered, and further work is ongoing.

3.2 Low-energy $e^+e^- \to \bar{p}p$ observables

Examining electromagnetic form factors (EMFF) of the proton (G_E and G_M) is an efficient way to probe the nucleon structure. The reaction $e^+e^- \to \bar{p}p$, and its inverse one $\bar{p}p \to e^+e^-$ (these two are related to each other by time reversal operation) are used to measure EMFF. The experiment shows a strong energy dependence in proton EMFF close to $\bar{p}p$ threshold. Recent measurements were done in Refs. [6, 7]. As shown above, at such energy region, the $\bar{p}p$ FSI plays an important role. And here in the $e^+e^- \to \bar{p}p$ decay, it is no exception. Taking into the fact that one photon exchange should dominate in the decay $e^+e^- \to \bar{p}p$, and thus the only allowed partial wave is the coupled ${}^3S_1 - {}^3D_1$. This provides an opportunity to make a (somewhat) clean prediction, compared to other decay channels where many partial waves are possible and maybe have a comparable significance. Including the coupled partial wave ${}^3S_1 - {}^3D_1$, one could extend Eq. (3.1) to a 2×2 matrix form

$$A_0 = \begin{pmatrix} A_0^{SS} & A_0^{SD} \\ A_0^{DS} & A_0^{DD} \end{pmatrix}, \quad T_{\bar{p}p} = \begin{pmatrix} T_{\bar{p}p}^{SS} & T_{\bar{p}p}^{SD} \\ T_{\bar{p}p}^{DS} & T_{\bar{p}p}^{DD} \end{pmatrix} \tag{3.3}$$

The matrix A_0, again as before, is the bare production amplitude without $\bar{p}p$ FSI, and is connected to the bare EMFF G_E^0 and G_M^0. At near-threshold region, they can be approximated as constant. And imposing the condition $G_E = G_M$ we have only one overall normalization constant. Concerning the $\bar{N}N$ potential used in this work, both the chiral potential constructed in Ref. [10] and Jülich model

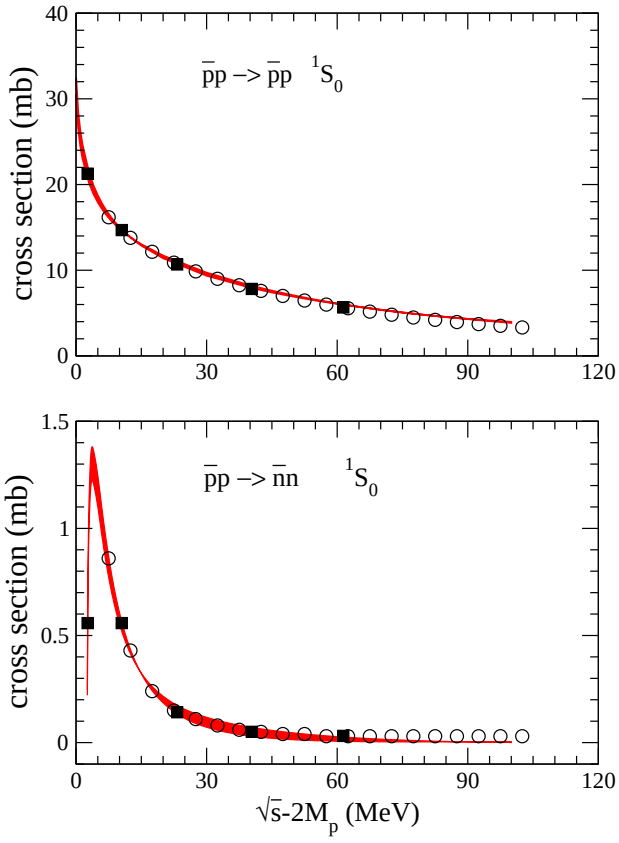

Figure 3: The $^1S_0$ partial-wave cross sections as a function of the excess energy. The squares represent the results for the published NNLO potential [10] with the cutoff combination {450 MeV, 500 MeV}. The circles indicate the cross sections for the partial-wave amplitudes of Ref. [3]. The bands show the results based on the refitted isospin-1 $^1S_0$ amplitudes.

A(OBE) [9] are considered. The results are shown in Fig. 4 for the cross section and effective form factor, where for the cross section we fitted to 60 MeV, and the effective form factor are calculated from the fitted overall constant. The ratio and the phase difference between the proton form factors G_E and G_M are also presented up to the same energy region as the cross section, see Ref. [19]. As can be seen, it reproduces the data rather well. We also calculate the differential cross section at a lower excess energy of 36.5 MeV, and the data is nicely reproduced, see Fig. 5. These altogether provide a good description of low-energy data on $e^+e^- \to \bar{p}p$, and thus strongly support our speculations of large $\bar{p}p$ FSI. In the reactions e^+e^- →multipions, $\bar{p}p$ is also shown to play an important role in the region [1750, 1950] MeV [20].

4. Summary

In summary, we have constructed and established a $\overline{N}N$ potential in chiral EFT. The resulting phase shifts and inelasticities agree with the partial-wave analysis reported in Ref. [3]. Scattering lengths and the level shift and widths of antiprotonic hydrogen are calculated, and they are in a good agreement with the experimental information within error bars. With such a $\overline{N}N$ interaction at hand,

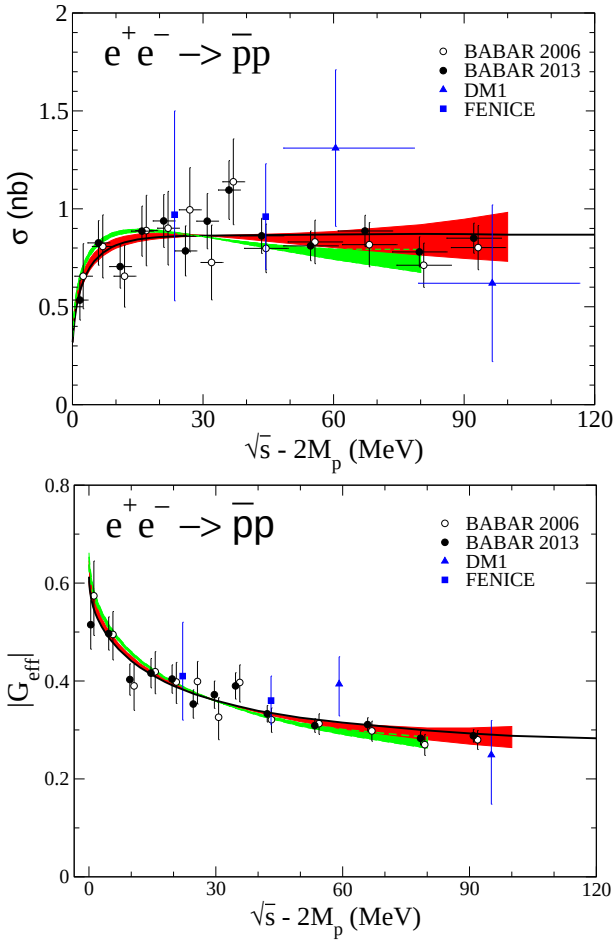

Figure 4: Cross section and effective form factor of the reaction $e^+e^- \to \bar{p}p$ as a function of the excess energy. The data are from the DM1 [17] (triangles), FENICE [18] (squares), and BaBar [6] (empty circles), [7] (filled circles) collaborations. The red/dark band shows results based on the $\overline{N}N$ amplitude of the chiral EFT interaction [10] up to NNLO while the green/light band are those for NLO. The solid line is the result for the $\overline{N}N$ amplitude predicted by the Jülich model A(OBE) [9]. The BaBar 2006 data are shifted to higher excess energy by 1 MeV.

we explored the $\bar{p}p$ FSI in several reactions. For $J/\psi \to \gamma\bar{p}p$ we perform a combined analysis of experimental events distribution and the $\bar{p}p$ partial-wave cross section ($^1S_0$ case). In order to describe the prominent peak shown in $J/\psi \to \gamma\bar{p}p$, we need a bound state in $^{31}S_0$. But the binding energy can not be well determined. The large $\bar{p}p$ FSI is also verified in $e^+e^- \to \bar{p}p$. The cross section and effective form factor up to the excess energy of 100 MeV are nicely reproduced. In all these processes, in fact, the whole energy dependences with the $\bar{p}p$ invariant mass spectrum come solely from the $\bar{p}p$ final-state interaction, since the bare production amplitude is approximated as constant without energy dependence.

Acknowledgement

We thank the organizers for providing the opportunity to present this work. Careful readings

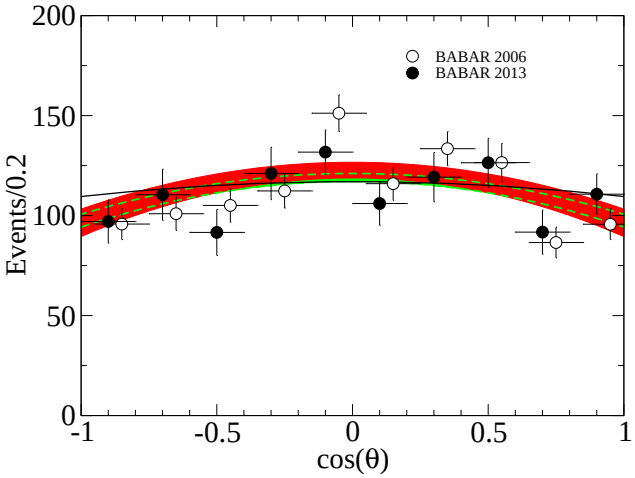

Figure 5: Differential cross section for $e^+e^- \to \bar{p}p$ at the excess energies of 36.5 MeV. The data are an average over [0, 73] MeV and are taken from Refs. [6, 7]. Same notations as in Fig. 4.

of Johann Haidenbauer and Ulf-G.Meißner are also specially acknowledged. This work is supported in part by the DFG and the NSFC through funds provided to the Sino-German CRC 110 "Symmetries and the Emergence of Structure in QCD".

References

[1] For a review, see e.g., E. Klempt, F. Bradamante, A. Martin and J. M. Richard, Phys. Rept. **368**, 119 (2002).

[2] E. Epelbaum, H. W. Hammer and U. G. Meißner, Rev. Mod. Phys. **81**, 1773 (2009) [arXiv:0811.1338 [nucl-th]].

[3] D. Zhou and R. G. E. Timmermans, Phys. Rev. C **86**, 044003 (2012) [arXiv:1210.7074 [hep-ph]].

[4] J. Z. Bai *et al.* [BES Collaboration], Phys. Rev. Lett. **91**, 022001 (2003) [hep-ex/0303006].

[5] M. Ablikim *et al.* [BESIII Collaboration], Phys. Rev. Lett. **108**, 112003 (2012) [arXiv:1112.0942 [hep-ex]].

[6] B. Aubert *et al.* [BaBar Collaboration], Phys. Rev. D **73**, 012005 (2006) [hep-ex/0512023].

[7] J. P. Lees *et al.* [BaBar Collaboration], Phys. Rev. D **87**, 092005 (2013) [arXiv:1302.0055 [hep-ex]].

[8] B. El-Bennich, M. Lacombe, B. Loiseau and S. Wycech, Phys. Rev. C **79**, 054001 (2009) [arXiv:0807.4454 [nucl-th]].

[9] T. Hippchen, K. Holinde and W. Plessas, Phys. Rev. C **39**, 761 (1989).

[10] X. W. Kang, J. Haidenbauer and U. G. Meißner, JHEP **1402**, 113 (2014) [arXiv:1311.1658 [hep-ph]].

[11] X. W. Kang, B. Kubis, C. Hanhart and U. G. Meißner, Phys. Rev. D **89**, 053015 (2014) [arXiv:1312.1193 [hep-ph]].

[12] E. Epelbaum, W. Glöckle and U. G. Meißner, Eur. Phys. J. A **19**, 125 (2004) [nucl-th/0304037].

[13] M. Ablikim *et al.* [BES Collaboration], Eur. Phys. J. C **53**, 15 (2008) [arXiv:0710.5369 [hep-ex]]; M. Ablikim *et al.* [BESIII Collaboration], Phys. Rev. D **87**, 112004 (2013) [arXiv:1303.3108 [hep-ex]].

[14] J. P. Alexander *et al.* [CLEO Collaboration], Phys. Rev. D **82**, 092002 (2010) [arXiv:1007.2886 [hep-ex]].

[15] J.-P. Dedonder, B. Loiseau, B. El-Bennich and S. Wycech, Phys. Rev. C **80**, 045207 (2009) [arXiv:0904.2163 [nucl-th]].

[16] X. W. Kang, J. Haidenbauer and U. G. Meißner, Phys. Rev. D **91**, 074003 (2015) [arXiv:1502.00880 [nucl-th]].

[17] B. Delcourt *et al.*, Phys. Lett. B **86**, 395 (1979).

[18] A. Antonelli *et al.*, Nucl. Phys. B **517**, 3 (1998).

[19] J. Haidenbauer, X.-W. Kang and U.-G. Meißner, Nucl. Phys. A **929**, 102 (2014) [arXiv:1405.1628 [nucl-th]].

[20] J. Haidenbauer, C. Hanhart, X. W. Kang and U. G. Meißner, Phys. Rev. D **92**, 054032 (2015) [arXiv:1506.08120 [nucl-th]].